PHOTONICS Research

Band-gap-tailored random laser

Hongbo Lu,[1,2] Jian Xing,[1] Cheng Wei,[1] Jiangying Xia,[3] Junqing Sha,[1] Yunsheng Ding,[2] Guobing Zhang,[1,2] Kang Xie,[3] Longzhen Qiu,[1,2] and Zhijia Hu[1,3,4,*]

[1]Key Laboratory of Special Display Technology, Ministry of Education, National Engineering Laboratory of Special Display Technology, State Key Laboratory of Advanced Display Technology, Academy of Opto-Electronic Technology, Hefei University of Technology, Hefei 230009, China
[2]Key Laboratory of Advanced Functional Materials and Devices of Anhui Province, School of Chemistry and Chemical Engineering, Hefei University of Technology, Hefei 230009, China
[3]School of Instrument Science and Opto-Electronics Engineering, Hefei University of Technology, Hefei 230009, China
[4]Aston Institute of Photonic Technologies, Aston University, Birmingham B4 7ET, UK
*Corresponding author: zhijiahu@hfut.edu.cn

Received 28 December 2017; revised 12 February 2018; accepted 12 February 2018; posted 13 February 2018 (Doc. ID 318385); published 18 April 2018

A band-gap-tailored random laser with a wide tunable range and low threshold through infrared radiation is demonstrated. When fluorescent dyes are doped into the liquid crystal and heavily doped chiral agent system, we demonstrate a wavelength tuning random laser instead of a side-band laser, which is caused by the combined effect of multi-scattering of liquid crystal (LC) and band-gap control. Through rotating the infrared absorbing material on the side of the LC cell, an adjustable range for random lasing of 80 nm by infrared light irradiation was observed.

OCIS codes: (230.3720) Liquid-crystal devices; (140.3600) Lasers, tunable.

https://doi.org/10.1364/PRJ.6.000390

1. INTRODUCTION

Random lasers (RLs), which result from the multiple scattering of light inside a disordered optical gain medium, have attracted a lot of attention during the last few decades for their potential applications as cheap, micro/nano-sized, low-coherence laser sources and displays [1,2]. In contrast to conventional lasers, RLs emit light at multiple wavelengths over a broad spatial emission profile due to the lack of a resonance cavity [3]. Therefore, the lasing features, such as position, direction, and wavelength, are unpredictable [4]. This means RLs are uncontrollable, which severely hinders their applicability in many practical circumstances. From an application point of view, an externally controlled RL is highly desirable. In recent reports, Gottardo *et al.* [5] showed that Mie resonances can control the peak wavelength of an RL. These Mie resonances introduce a wavelength-dependent diffusion constant. The diffuse analog of the cavity decay time will therefore become wavelength-dependent, which enables control over the emission wavelength of an RL. El-Dardiry *et al.* [6] achieved experimental control over the emission wavelength of an RL by adjusting the emission light absorption amount. They provided an alternative and much easier route for tailoring intrinsically disordered lasers through controlling over the absorption amount at the emission wavelength.

Nowadays, liquid crystals (LCs) are widely used in display technologies and opto-electronic fields—such as in superior light modulators and dye-doped LC (DDLC) lasers [7]. LCs are also superior light scatterers and excellent candidates for generating random lasing due to their intrinsic birefringence characteristics. In previous reports, different types of LCs—such as nematic LCs (NLCs) [8–10], cholesteric LCs (CLCs) [11–13], and polymer-dispersed LCs (PDLCs) [14]—have been used as scattering media to investigate RL characteristics. Meanwhile, LCs have been considered for use as the host materials in RLs, because they can be easily modulated by external factors such as temperature [15–17], electric fields [18–20], and light fields [21,22]. Yoshida *et al.* [23] studied a wavelength-swept lasing system produced from a single free-standing film. They presented a simple fabrication method in which a network of nano-pores was formed in a photopolymerized CLC film, and wavelength tuning was demonstrated in a CLC based on refractive index modulation.

CLCs have received a great deal of attention in photonics because they are available in a variety of textures with unique optical properties including the planar texture, focal conic texture, and homeotropic texture, etc. In the planar texture, CLCs can be treated as a class of one-dimensional photonic crystals with an easily tailored band gap determined by the pitch and average refractive index. Lasing will be found at the edge band

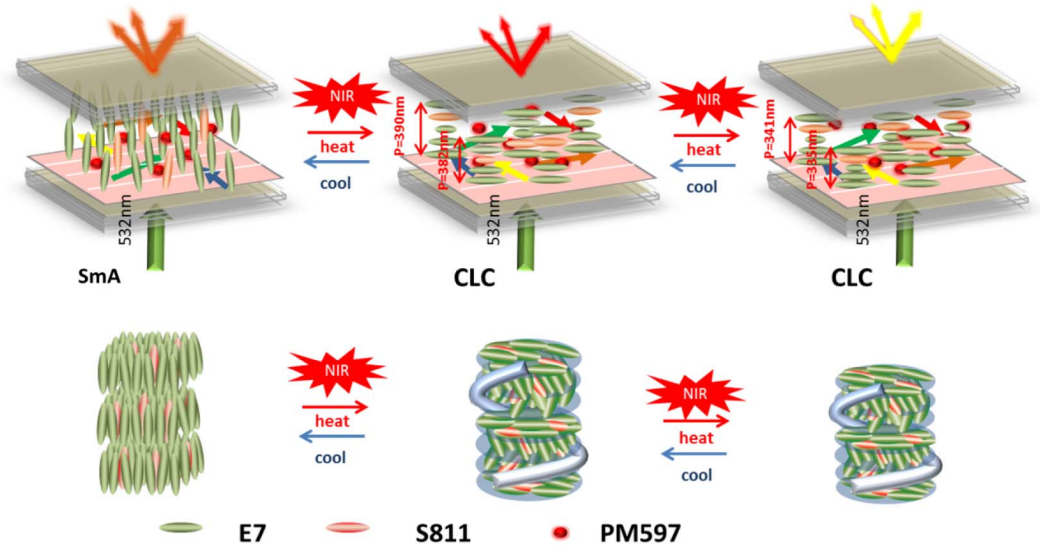

Fig. 1. Schematic of the band-gap-tailored random laser.

under sufficient pumping conditions; this is the so-called band-edge CLC laser. In the focal conic texture, CLCs are equivalent to a strong scattering medium with random helical structures, have a low diffusion constant and are therefore good media for random lasing. In the homeotropic texture, CLCs cannot be used as the scattering medium for DDLC lasers because the LC molecules are neatly arranged. Morris *et al.* [24] achieved the switch between band-edge laser emission and RL emission using an electric field. At low frequencies, the CLC exhibits a dynamic scattering/turbulent state, and at higher frequencies the CLC exhibits a planar texture. There has been little research on DDLC wavelength control in RLs, but the ability to tune the band-edge laser emission can be achieved based on the tunable band gap in CLC. Lin *et al.* [25] reported on a band-edge laser with a tuning range over 100 nm at the band edges of the CLC photonic band gap through using photo-tunable chiral materials AzoB. Unfortunately, the light sources used in these references are high-energy ultraviolet (UV) light and that might result in material damage, environmental contamination, or poor penetrated length through container substrates. Near-infrared (NIR) light would be much more applicable in fields such as life sciences, drug delivery, materials science, and aerospace because of its invisibility and outstanding penetration for temporal and spatial remote activation of materials [26]. Thus, it is crucial to develop NIR-light-controlled CLC-based lasers.

Tzeng *et al.* [27] observed a transition from the smectic A phase to the cholesteric phase in a heavily doped nematic system. Furthermore, they observed a sensitive band-gap tuning in the cholesteric phase with changing temperature. In this work, we obtain NIR light control of the transition from the smectic phase to a cholesteric phase. We accomplish this through the infrared light thermal effect by rotating the infrared absorbing material on the side of the LC cell for the mixed solution of nematic liquid crystal E7 and heavily doped chiral agent S811. Thus, we demonstrate infrared light control of a CLC band gap over a range from 500 to 700 nm for the first time to our knowledge. Interestingly, when we dope fluorescent dyes and the heavily doped chiral agent into the LC system, we demonstrate the wavelength tuning RL instead of the side-band laser, which is caused by the combined effect of multi-scattering of LC and band-gap control (Fig. 1). Here, for the first time to the best of our knowledge, we report on a wide-wavelength-range tunable LC random lasing with a low threshold based on band-gap feedback through NIR light irradiation. The influence of different concentrations of absorbing materials, as well as different intensities and wavelengths of NIR on the regulatory ability of RLs, is researched.

2. EXPERIMENTAL SECTION

A. Materials

The CLC is a mixture of nematic LC E7 (HCCH, China) and chiral dopant S811 (Chengzhi Yonghua). The physical properties of E7 are as follows: $\Delta\varepsilon = 11.4$ at 1 kHz and 25°C, $\Delta n = 0.223$ at $\lambda = 589$ nm, and clearing temperature $T_c = 59.2$°C. A previously reported by our donor–acceptor (D–A), conjugated, low-band-gap polymer based on bithiophene and bis (2-oxoindolin-3-ylidene)-benzodifuran-dione (BIBDF), namely, PBIBDF-BT, was used as a near-infrared absorbing material and synthesized in our previous work [28]. The laser dye Pyrromethene 597 (PM597) by excition has a high quantum efficiency with only a small amount of non-radiative charge transfer between the dye molecules and the solvent energy level, which is advantageous for laser generation. In this paper, the mass fraction of PM597 is 1%. The structure of the infrared absorbing material (PBIBDF-BT), chiral agent (S811), and PM597 are shown in Fig. 2.

B. Preparation of Samples

The materials used in CLC in terms of the mass fraction are 30% S811 and 70% E7. The thermotropic and optical properties of the mixed solution of NLC E7 and chiral agent S811 were investigated using differential scanning calorimetry and optical microscopy, respectively.

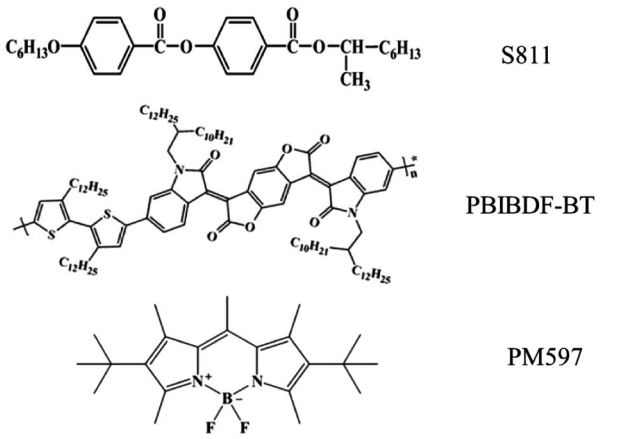

Fig. 2. Chemical structures of chiral agent S811, infrared absorbing material PBIBDF-BT, and laser dye PM597.

The mixture solution of polymethyl methacrylate (PMMA) and PBIBDF-BT was prepared and spin-coated on the inside of a quartz glass plate to uniformly form a film. To fabricate the defect CLC, we only made a uniform-oriented friction on the thin film with the brush, which then was to form the LC cell with the other glass plate. The LC cell thickness was controlled by 40-μm dispersion of spacer beads. The weight ratio between E7 and S811 was kept at ~7:3, and they were then injected into an empty cell by capillarity action.

The experimental setup to measure the random lasing emission spectrum of the dye-doped chiral NLC is shown in Fig. 3. One pumped laser beam is derived from a *Q*-switched Nd:YAG second-harmonic-generation pulse laser (wavelength of 532 nm, pulse duration of 10 ns, and repetition rate of 10 Hz). The pump pulse energy and polarization are controlled by a Glan prism group. The pump beam is used to excite the dye-doped chiral NLC sample with the NIR irradiation. The emitted light along the CLC axis is collected by a fiber spectrometer (QE65PRO, Ocean Optics, resolution ~0.4 nm, integration time 100 ms). The diameter of the pump beam on the sample is about 100 μm.

3. RESULTS AND DISCUSSION

The thermotropic and optical properties of the NLC E7 and chiral agent S811 solution were investigated using differential scanning calorimetry [DSC, Fig. 4(a)] and optical microscopy [POM, Fig. 4(b)], respectively. Note that two different LC

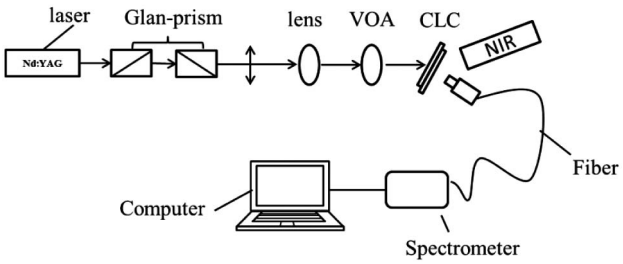

Fig. 3. Experimental setup for the NIR controlling random laser.

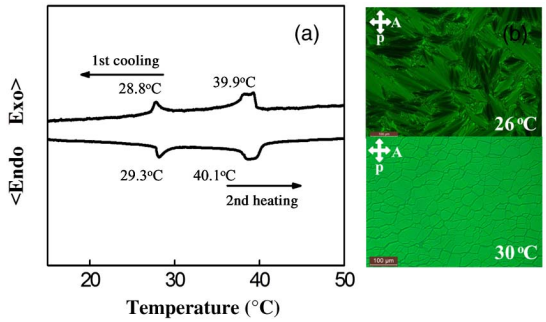

Fig. 4. (a) DSC curves of CLC-based S811 (30 wt.%) in E7 (70 wt.%) at heating/cooling rate of 1°C per minute; (b) LC textures recorded under crossed polarizers for the sample at 26°C and 30°C.

phases were enantiotropically observed in both heating and cooling cycles from the DSC results, which is confirmed by the appearance of a cholesteric phase and smectic A phase in the POM image.

Figure 5(a) shows the transmission spectra for the prepared CLC cells mounted in a heated stage over different temperatures. The band gap exhibits a redshift effect with decreasing temperature. The bandwidth also widens with the redshift of the central wavelength, which is entirely consistent with the formula $\Delta\lambda = p \times (n_e - n_o)$, where $\Delta\lambda$ is the bandwidth of the band gap, p is the pitch of the CLC, n_o is the ordinary refractive index, and n_e is the extraordinary optical refractive index. Figure 5(b) shows the band-gap change for different 850-nm irradiation times at an intensity of 30 mW·cm^{-2}. Note that the central wavelength of the reflection band

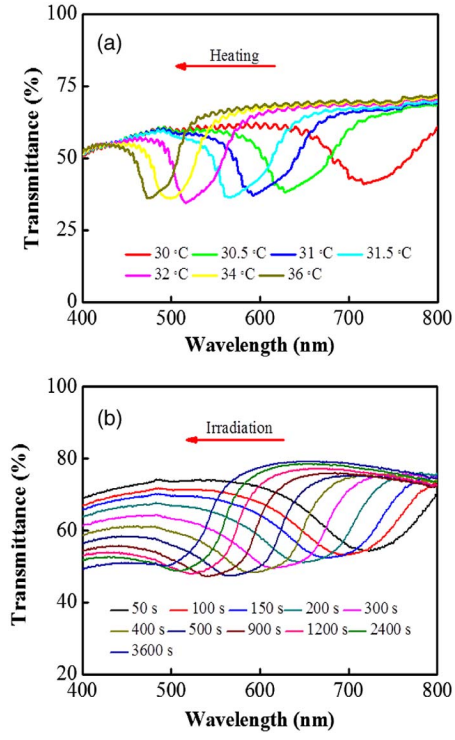

Fig. 5. Transmission spectra of CLC as functions of (a) temperature and (b) irradiation time at 850 nm.

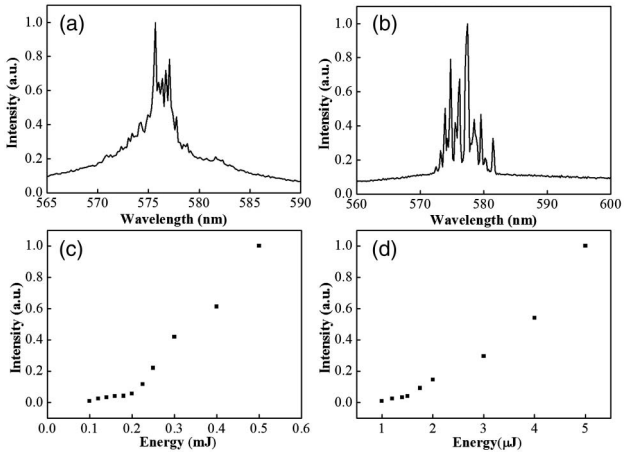

Fig. 6. Random lasing emission (a) for smectic A state at ~0.35 mJ pump intensity, and (b) for cholesteric state at ~3 μJ pump intensity; the relation between the output intensity and the pump intensity for (c) smectic A state and (d) cholesteric state.

is 700 nm when the NIR irradiation time is roughly 50 s. The central wavelength of the band gap exhibits a blueshift with increasing irradiation time and stabilizes at roughly 500 nm after 3600 s. Therefore, we successfully achieved a tunable band gap of more than 200 nm by NIR irradiation.

We measured the random lasing emission in the smectic A and cholesteric phases as shown in Figs. 6(a) and 6(b). There are several sharp emission peaks with a full width at half-maximum (FWHM) in the smectic A phase and cholesteric phase less than 0.2 nm and 1 nm, respectively. The relationship between the output intensity and the pump intensity for these two different LC states is also shown in Figs. 6(c) and 6(d). The thresholds for the smectic A state and the cholesteric state are 0.2 mJ and 1.5 μJ, respectively. When the pump intensity is below the threshold, the emission spectra are dominated by spontaneous emission of the laser dye. RLs can be obtained when the pump energy is above the threshold. The threshold of the cholesteric state is almost two orders of magnitude lower than that of the smectic A state. The arrangement of LC molecules in the smectic A state is ordered, and the structure of LC molecule in the cholesteric state is partially ordered. Thus, the scattering for smectic A phases of LCs is weaker than that of cholesteric phases. Meanwhile, the band-gap feedback of CLCs also boosts the emission of RLs. Therefore, the threshold for the cholesteric phase is lower than that of the smectic A phase.

Figure 7 shows the random lasing spectra of LCs at the cholesteric state at different NIR (850-nm) irradiation times. After three minutes of irradiation, the LC state changes from the smectic A to the CLC planar texture. The lasing spectra are around 640 nm and the RL peak wavelength blueshifts ~80 nm as the illumination time increases to 24 min. When the infrared light is removed, the RL wavelength redshifts as shown in Fig. 8. In previous reports, only the band-edge laser has been obtained in the planar texture of CLC [29–31]. Interestingly, we observe RLs and not band-edge lasers in the planar texture of the CLC. In our experiment, we make a friction orientation layer on one side of the LC cell; thus, a

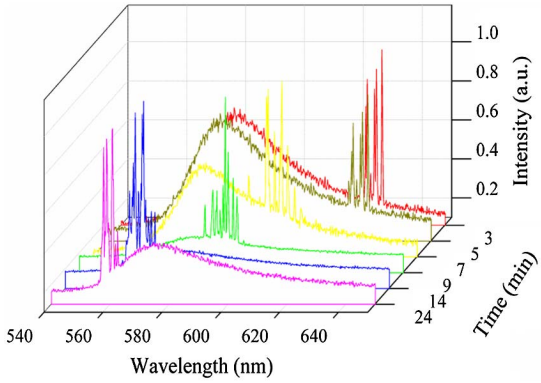

Fig. 7. Random lasing spectra of LCs at the cholesteric state at different NIR (850-nm) irradiation times.

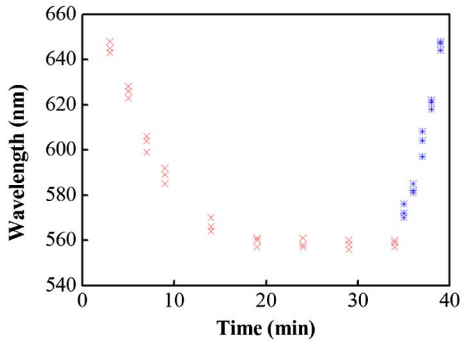

Fig. 8. Random laser wavelength changes with time (× represents three major laser peaks of the RL with NIR irradiation. ∗ represents three major laser peaks of the RL without NIR light).

defective planar texture of the CLC is formed. When a beam of pump light is incident on the sample, the defective planar texture causes multi-scattering to form RL emission. Moreover, the band-gap feedback in the planar texture causes reflection of the fixed wavelength. Therefore, two effects boost the tunable RL in the planar texture of the cholesteric phase.

We also show a band-gap change for 940-nm NIR light irradiation at an intensity of 30 $mW \cdot cm^{-2}$ in Fig. 9. Similarly, the band-gap central wavelength is 700 nm when the 940-nm NIR irradiation time is roughly 50 s. The band-gap central wavelength blueshifts with increasing irradiation time and stabilizes at roughly 550 nm after irradiating for 7000 s. However, we find it is interesting that the final stable wavelength is different from that at 850-nm NIR illumination. The PBIBDF-BT absorptivity at 850 nm is stronger than that at 940 nm, which results in a high increasing temperature speed and heat balance temperature. Thus, two different NIR irradiation wavelengths affect the final stabilized band-gap wavelength of the cholesteric planar texture. Therefore, we study the stabilized RL wavelength at different NIR irradiations, as shown in Fig. 10(a). For 850-nm and 940-nm irradiation, the maximum peak of the RL is stable at 557 nm and 569 nm, respectively. This proves that the CLC band-gap shift can control the random lasing emission. Meanwhile, the PBIBDF-BT concentration

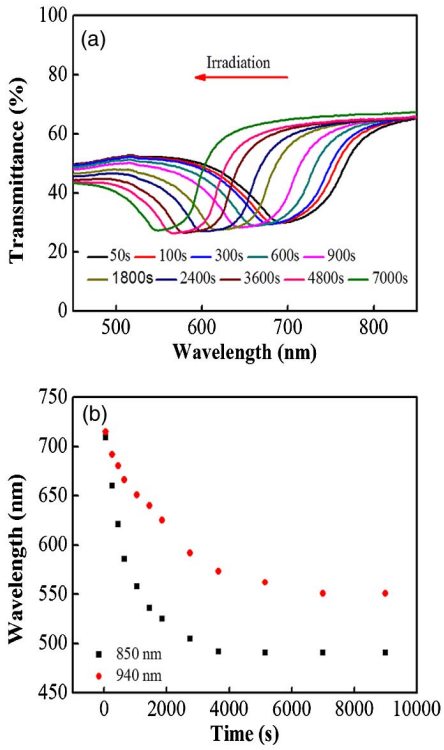

Fig. 9. (a) Transmission spectra of CLC as a function of irradiation time of 940-nm NIR. (b) Bragg wavelength as a function of NIR irradiation time. (■ 850-nm NIR irradiation on the sample; • 940-nm NIR irradiation on the sample.)

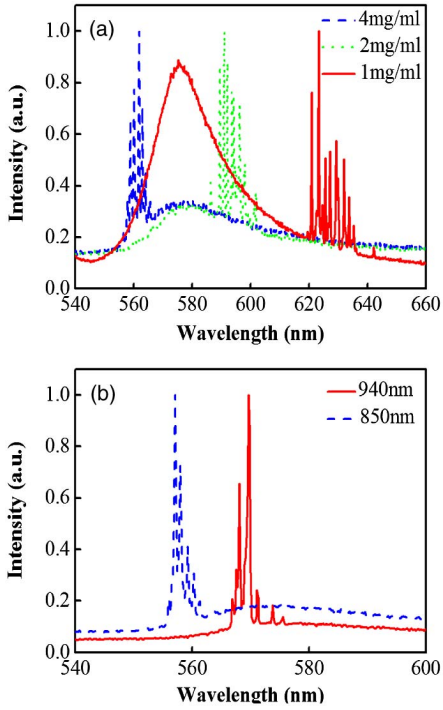

Fig. 10. Stable random lasing wavelength for (a) different NIR irradiation wavelengths and (b) different concentrations of infrared absorbing material at 850 nm for 30 min.

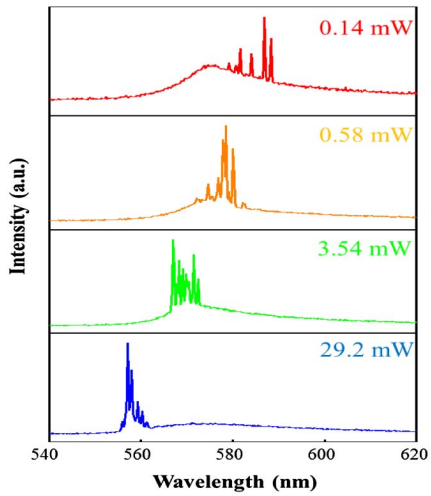

Fig. 11. Stabilized wavelength of RLs changes with varying NIR irradiation power.

affects the NIR light energy absorption, which affects the temperature of the heat balance and the CLC band-gap-stabilized wavelength. Therefore, we studied the stabilized wavelength of RL changes with different concentrations of PBIBDF-BT, as shown in Fig. 10(b). For low concentrations of the PBIBDF-BT sample, the RL wavelength stabilizes around 620 nm. As the concentration of PBIBDF-BT increases from 1 to 4 mg/mL, the stabilized wavelength of the RL blueshifts 60 nm from 623 nm to 561 nm.

Similarly, the NIR irradiation power also influences the heat balance, which affects the wavelength of the CLC band gap. The RL-stabilized wavelength can be controlled by the NIR irradiation power, as shown in Fig. 11. As the light intensity increases, the RL-stabilized wavelength shifts from 586 to 557 nm. Therefore, we can simply achieve a range of random lasing wavelength emissions through NIR irradiation, which paves the way to control RLs and apply them in the display field.

4. CONCLUSIONS

To summarize, we obtain a band-gap tailored random laser with a wide tunable range and low threshold through infrared radiation. A simple fabrication method for defect CLC involving rotating the infrared absorbing material on the side of the liquid crystal cell is presented. The working mechanism has been well described: multiple scattering of defective planar texture of cholesteric phase to boost a random laser that is tailored by the band gap. We envision that tunable liquid crystals with the low-threshold random lasers demonstrated in this work may open a window to future RL applications in the laser display and optical communication fields.

Funding. Natural Science Foundation of Anhui Province, China (1708085MF150); National Natural Science Foundation of China (NSFC) (61107014, 51573036, 11404087, 11574070); China Postdoctoral Science Foundation (2015M571918, 2017T100442); H2020 Marie Skłodowska-Curie Actions (MSCA) (744817); Fundamental Research

Funds for the Central Universities, China (JD2017JGPY0006, JZ2017HGTB0187, PA2017GDQT0024).

REFERENCES

1. S. Xiao, Q. Song, F. Wang, L. Liu, J. Liu, and L. Xu, "Switchable random laser from dye-doped polymer dispersed liquid crystal waveguides," IEEE J. Quantum. Electron. **43**, 407–410 (2007).
2. I. M. Vellekoop and A. P. Mosk, "Focusing coherent light through opaque strongly scattering media," Opt. Lett. **32**, 2309–2311 (2007).
3. J. H. Lin and Y. L. Hsiao, "Manipulation of the resonance characteristics of random lasers from dye-doped polymer dispersed liquid crystals in capillary tubes," Opt. Mater. Express **4**, 1555–1563 (2014).
4. M. Leonetti, C. Conti, and C. López, "Tunable degree of localization in random lasers with controlled interaction," Appl. Phys. Lett. **101**, 051104 (2012).
5. S. Gottardo, R. Sapienza, P. D. García, A. Blanco, D. S. Wiersma, and C. López, "Resonance-driven random lasing," Nat. Photonics **2**, 429–432 (2008).
6. R. G. S. El-Dardiry and A. Lagendijk, "Tuning random lasers by engineered absorption," Appl. Phys. Lett. **98**, 161106 (2011).
7. L. J. Chen, J. D. Lin, S. Y. Huang, T. S. Mo, and C. R. Lee, "Thermally and electrically tunable lasing emission and amplified spontaneous emission in a composite of inorganic quantum dot nanocrystals and organic cholesteric liquid crystals," Adv. Opt. Mater. **1**, 637–643 (2013).
8. L. Ye, Y. Wang, Y. Feng, C. Zhao, and G. Hu, "Study of low-threshold and high-intensity random lasing in dye doped liquid crystals," J. Laser Appl. **28**, 022005 (2016).
9. F. Yao, W. Zhou, H. Bian, Y. Zhang, Y. Pei, X. Sun, and Z. Lv, "Polarization and polarization control of random lasers from dye-doped nematic liquid crystals," Opt. Lett. **38**, 1557–1559 (2013).
10. L. Ye, C. Zhao, Y. Feng, B. Gu, Y. Cui, and Y. Lu, "Study on the polarization of random lasers from dye-doped nematic liquid crystals," Nanoscale Res. Lett. **12**, 27 (2017).
11. B. He, Q. Liao, and Y. Huang, "Random lasing in a dye doped cholesteric liquid crystal polymer solution," Opt. Mater. **31**, 375–379 (2008).
12. C. W. Chen, H. C. Jau, C. T. Wang, C. H. Lee, I. C. Khoo, and T. H. Lin, "Random lasing in blue phase liquid crystals," Opt. Express **20**, 23978–23984 (2012).
13. L. Li and L. Deng, "Low threshold and coherent random lasing from dye-doped cholesteric liquid crystals using oriented cells," Laser Phys. **23**, 085001 (2013).
14. S. Gottardo, S. Cavalieri, O. Yaroshchuk, and D. S. Wiersma, "Quasi-two-dimensional diffusive random laser action," Phys. Rev. Lett. **93**, 263901 (2004).
15. K. Funamoto, M. Ozaki, and K. Yoshino, "Discontinuous shift of lasing wavelength with temperature in cholesteric liquid crystal," Jpn. J. Appl. Phys. **42**, L1523–L1525 (2003).
16. S. M. Morris, A. D. Ford, M. N. Pivnenko, and H. J. Coles, "Enhanced emission from liquid-crystal lasers," J. Appl. Phys. **97**, 023103 (2005).
17. Y. Huang, Y. Zhou, C. Doyle, and S. T. Wu, "Tuning the photonic band gap in cholesteric liquid crystals by temperature-dependent dopant solubility," Opt. Express **14**, 1236–1242 (2006).
18. S. Furumi, S. Yokoyama, A. Otomo, and S. Mashiko, "Electrical control of the structure and lasing in chiral photonic band-gap liquid crystals," Appl. Phys. Lett. **82**, 16–18 (2003).
19. M. Kasano, M. Ozaki, K. Yoshino, and W. Haase, "Electrically tunable waveguide laser based on ferroelectric liquid crystal," Appl. Phys. Lett. **82**, 4026–4028 (2003).
20. B. Park, M. Kim, S. W. Kim, W. Jang, H. Takezoe, Y. Kim, E. H. Choi, Y. H. Seo, G. S. Cho, and S. O. Kang, "Electrically controllable omnidirectional laser emission from a helical-polymer network composite film," Adv. Mater. **21**, 771–775 (2009).
21. G. Chanishvili, G. Chilaya, R. Petriashvili, R. Barberi, R. Bartolino, G. Cipparrone, A. Mazzulla, and L. Oriol, "Phototunable lasing in dye-doped cholesteric liquid crystals," Appl. Phys. Lett. **83**, 5353–5355 (2003).
22. P. V. Shibaev, R. L. Sanford, D. Chiappetta, V. Milner, A. Genack, and A. Bobrovsky, "Light controllable tuning and switching of lasing in chiral liquid crystals," Opt. Express **13**, 2358–2363 (2005).
23. Y. Inoue, H. Yoshida, K. Inoue, Y. Shiozaki, H. Kubo, A. Fujii, and M. Ozaki, "Tunable lasing from a cholesteric liquid crystal film embedded with a liquid crystal nanopore network," Adv. Mater. **23**, 5498–5501 (2011).
24. S. M. Morris, D. J. Gardiner, P. J. W. Hands, M. M. Qasim, T. D. Wilkinson, I. H. White, and H. J. Coles, "Electrically switchable random to photonic band-edge laser emission in chiral nematic liquid crystals," Appl. Phys. Lett. **100**, 071110 (2012).
25. T. H. Lin, Y. J. Chen, C. H. Wu, Y. G. Fuh, J. H. Liu, and P. C. Yang, "Cholesteric liquid crystal laser with wide tuning capability," Appl. Phys. Lett. **86**, 161120 (2005).
26. L. Wang, H. Dong, Y. Li, R. Liu, Y. F. Wang, H. K. Bisoyi, L. D. Sun, C. H. Yan, and Q. Li, "Luminescence-driven reversible handedness inversion of self-organized helical superstructures enabled by a novel near-infrared light nanotransducer," Adv. Mater. **27**, 2065–2069 (2015).
27. S. Y. T. Tzeng, C. N. Chen, and Y. Tzeng, "Thermal tuning band gap in cholesteric liquid crystals," Liq. Cryst. **37**, 1221–1224 (2010).
28. G. Zhang, P. Li, L. Tang, J. Ma, X. Wang, H. Lu, B. Kang, K. Cho, and L. Qiu, "A bis(2-oxoindolin-3-ylidene)-benzodifuran-dione containing copolymer for high-mobility ambipolar transistors," Chem. Commun. **50**, 3180–3183 (2014).
29. C. Mowatt, S. M. Morris, M. H. Song, T. D. Wilkinson, R. H. Friend, and H. J. Coles, "Comparison of the performance of photonic band-edge liquid crystal lasers using different dyes as the gain medium," J. Appl. Phys. **107**, 043101 (2010).
30. Z. G. Zheng, B. W. Liu, L. Zhou, W. Wang, W. Hu, and D. Shen, "Wide tunable lasing in photoresponsive chiral liquid crystal emulsion," J. Mater. Chem. C **3**, 2462–2470 (2015).
31. V. I. Kopp, B. Fan, H. K. M. Vithana, and A. Z. Genack, "Low-threshold lasing at the edge of a photonic stop band in cholesteric liquid crystals," Opt. Lett. **23**, 1707–1709 (1998).